Supplementary material for the manuscript

Structural Chemistry & Number Theory Amalgamized: The Crystal Structure of $Na_{11}Hg_{52}$

authored by

Wolfgang Hornfeck and *Constantin Hoch*

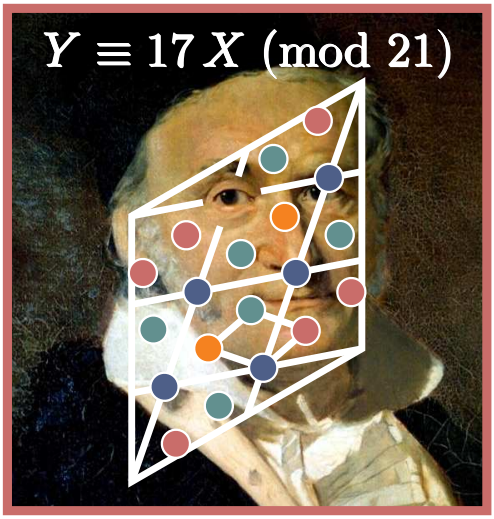

Gaussian spectacles The remarkably complex crystal structure of the sodium amalgam $Na_{11}Hg_{52}$ is best described via group-theoretic sublattices which are generated and concisely represented, including their point group symmetry, by number-theoretic formulas taken from the field of modular arithmetic developed by Gauss.

Contents

1 Description of the crystal structure of $Na_{11}Hg_{52}$ in terms of multiplicative congruential generators (MCGs)

The following sections contain selected information about the MCGs used for the description of the crystal structure of $Na_{11}Hg_{52}$. Given are the sublattice index identical to the modulus of the MCG, $T(\alpha, \beta) = M$, followed by its formula $Y = m\,X \pmod M$ with respect to integer coordinates (X, Y). Fractional coordinates of the sublattice nodes are obtained as $(x, y) = (X, Y)/M$. Finally, each MCG is explicitely stated in its canonical ordering of cycles.

1.1 MCGs used

1.1.1 P/P'-layers, Na- & non-rotated Hg-substructure of $F1/F2$-layers

$T(14, 1) = 183$; $Y \equiv 14\,X \pmod{183}$;
List of generators : $\{1, \cdots, 12, 16, \cdots, 24, 31, \cdots, 36, 46, \cdots, 48, 61\}$;

(0)(1 14 13 182 169 170)(2 28 26 181 155 157)(3 42 39 180 141 144)(4 56 52 179 127 131)
(5 70 65 178 113 118)(6 84 78 177 99 105)(7 98 91 176 85 92)(8 112 104 175 71 79)
(9 126 117 174 57 66)(10 140 130 173 43 53)(11 154 143 172 29 40)(12 168 156 171 15 27)
(16 41 25 167 142 158)(17 55 38 166 128 145)(18 69 51 165 114 132)(19 83 64 164 100 119)
(20 97 77 163 86 106)(21 111 90 162 72 93)(22 125 103 161 58 80)(23 139 116 160 44 67)
(24 153 129 159 30 54)(31 68 37 152 115 146)(32 82 50 151 101 133)(33 96 63 150 87 120)
(34 110 76 149 73 107)(35 124 89 148 59 94)(36 138 102 147 45 81)(46 95 49 137 88 134)
(47 109 62 136 74 121)(48 123 75 135 60 108)(61 122)

1.1.2 Na-substructure of $F1/F2$-layers

$T(9, 5) = 61$; $Y \equiv 14\,X \pmod{61}$;
List of generators : $\{1, \cdots, 4, 6, \cdots, 8, 11\ \&\ 12, 16\}$;

(0)(1 14 13 60 47 48)(2 28 26 59 33 35)(3 42 39 58 19 22)(4 56 52 57 5 9)
(6 23 17 55 38 44)(7 37 30 54 24 31)(8 51 43 53 10 18)(11 32 21 50 29 40)
(12 46 34 49 15 27)(16 41 25 45 20 36)

1.1.3 Rotated Hg-substructure of $F1/F2$-layers

$T(15, 7) = 169$; $Y \equiv 147\,X \pmod{169}$;
List of generators : $\{1, \cdots, 7, 9, \cdots, 14, 17, \cdots, 21, 25, \cdots, 28, 33, \cdots, 35, 41\ \&\ 42, 49\}$;

(0)(1 147 146 168 22 23)(2 125 123 167 44 46)(3 103 100 166 66 69)(4 81 77 165 88 92)
(5 59 54 164 110 115)(6 37 31 163 132 138)(7 15 8 162 154 161)(9 140 131 160 29 38)
(10 118 108 159 51 61)(11 96 85 158 73 84)(12 74 62 157 95 107)(13 52 39 156 117 130)
(14 30 16 155 139 153)(17 133 116 152 36 53)(18 111 93 151 58 76)(19 89 70 150 80 99)
(20 67 47 149 102 122)(21 45 24 148 124 145)(25 126 101 144 43 68)(26 104 78 143 65 91)
(27 82 55 142 87 114)(28 60 32 141 109 137)(33 119 86 136 50 83)(34 97 63 135 72 106)
(35 75 40 134 94 129)(41 112 71 128 57 98)(42 90 48 127 79 121)(49 105 56 120 64 113)

1.2 Site occupancy schemes of $F1/F2$-layers

In the following we give some detailed information about the site occupancy scheme as it is occurring in the flat layers, $F1/F2$, of the crystal structure of $Na_{11}Hg_{52}$. In particular, we thereby establish a concordance between:

1. The cycle structure of the multiplicative congruential generator $Y \equiv 14\,X \pmod{183}$,
2. its expansion into integral coordinate pairs $(X \;\; Y)_{F2}^{F1}$, and
3. the site-specific chemical decoration of the two distinct flat layers with the elements Na ($\circ$) and Hg ($\bullet$), including their occurrence on the same site with mixed occupancy ($\circ/\bullet$) or the presence of vacancies ($\square$).

As before, fractional coordinates are obtained as: $(x, y) = (X, Y)/M$ where $M = 183$.

Moreover, the site occupancy scheme is given in two representations,

1. A 'circular twist' one, in which sites are arranged according to the one-line cycle representation of an MCG, and
2. a 'linear shift' one, in which sites are arranged according to the two-line matrix representation of an MCG.

Both representations highlight distinct features of the structure, regarding the observed distribution of atoms and vacancies. The 'circular twist' representation, for instance, matches the crystallographic orbits, i.e. the splitting of sublattice sites according to space group symmetry. Listing the coordinate pairs $(X \;\; Y)_{F2}^{F1}$ in a 'linear shift' fashion, on the other hand, reveals a general distribution pattern

$$(X_i, Y_i)^{\circ}_{\square}(X_{i+1}, Y_{i+1})^{\square}_{\circ}(X_{i+2}, Y_{i+2})^{\bullet}_{\square}/^{\square}_{\bullet}$$

for the site occupancies of successive triples, starting from the origin, which may have been left unnoticed otherwise.

The numerous (colour-coded) exceptions to this general distribution pattern, which are responsible for the lion's share of the structural complexity of $Na_{11}Hg_{52}$, are due to vacancy formation ($\circ \to \square$ or $\bullet \to \square$), while only a few ones are related to a distinct chemical ordering (always $\circ \to \bullet$, never $\bullet \to \circ$). Yet still 115 out of 183 sites (62.8%) match the expected atomic species distribution pattern, i.e. $(Na_2Hg)_{61}$, for the combined flat layers along a torus line starting from the origin and proceeding along the $[1, 14, 0]$ direction.

Finally, from yet another point of view, a more conventional group–subgroup scheme covers the splitting of Wyckoff positions and the accompanying hierarchical evolution of the site occupancies as resulting from a sequence of symmetry reduction steps, starting from a hexagonal primitive aristotype structure. Here, the site occupancy scheme observed for $Na_{11}Hg_{52}$ turns out to be the outcome of a chemically meaningful ordering along the line

$$Na/Hg \to NaHg \to Na_2Hg \to NaHg_5 \to \ldots$$

up to the introduction of vacancies yielding the actual crystal structure of $Na_{11}Hg_{52}$.

1.2.1 Site occupancy scheme in 'circular twist' representation

$(X\ \ Y)_{F2}^{F1}$	$Y \equiv 14\,X \pmod{183}$
$(0\ \ 0)^{\bullet}_{\square}$	(0)
$(1\ \ 14)^{\square}_{\circ}(14\ \ 13)^{\bullet}_{\square}(13\ \ 182)^{\square}_{\circ}(182\ \ 169)^{\bullet}_{\square}(169\ \ 170)^{\square}_{\circ}(170\ \ 1)^{\bullet}_{\square}$	(1 14 13 182 169 170)
$(2\ \ 28)^{\square}_{\square}(28\ \ 26)^{\square}_{\circ}(26\ \ 181)^{\square}_{\square}(181\ \ 155)^{\square}_{\circ}(155\ \ 157)^{\square}_{\square}(157\ \ 2)^{\square}_{\circ}$	(2 28 26 181 155 157)
$(3\ \ 42)^{\square}_{\square}(42\ \ 39)^{\circ}_{\square}(39\ \ 180)^{\square}_{\square}(180\ \ 141)^{\circ}_{\square}(141\ \ 144)^{\square}_{\square}(144\ \ 3)^{\circ}_{\square}$	(3 42 39 180 141 144)
$(4\ \ 56)^{\square}_{\circ}(56\ \ 52)^{\bullet}_{\square}(52\ \ 179)^{\square}_{\circ}(179\ \ 127)^{\bullet}_{\square}(127\ \ 131)^{\square}_{\circ}(131\ \ 4)^{\bullet}_{\square}$	(4 56 52 179 127 131)
$(5\ \ 70)^{\square}_{\bullet}(70\ \ 65)^{\square}_{\circ}(65\ \ 178)^{\square}_{\bullet}(178\ \ 113)^{\square}_{\circ}(113\ \ 118)^{\square}_{\bullet}(118\ \ 5)^{\square}_{\circ}$	(5 70 65 178 113 118)
$(6\ \ 84)^{\circ}_{\square}(84\ \ 78)^{\square}_{\square}(78\ \ 177)^{\circ}_{\square}(177\ \ 99)^{\square}_{\square}(99\ \ 105)^{\circ}_{\square}(105\ \ 6)^{\square}_{\square}$	(6 84 78 177 99 105)
$(7\ \ 98)^{\square}_{\circ}(98\ \ 91)^{\square}_{\square}(91\ \ 176)^{\square}_{\circ}(176\ \ 85)^{\square}_{\square}(85\ \ 92)^{\square}_{\circ}(92\ \ 7)^{\square}_{\square}$	(7 98 91 176 85 92)
$(8\ \ 112)^{\square}_{\bullet}(112\ \ 104)^{\square}_{\circ}(104\ \ 175)^{\square}_{\bullet}(175\ \ 71)^{\square}_{\circ}(71\ \ 79)^{\square}_{\bullet}(79\ \ 8)^{\square}_{\circ}$	(8 112 104 175 71 79)
$(9\ \ 126)^{\circ}_{\square}(126\ \ 117)^{\circ}_{\square}(117\ \ 174)^{\circ}_{\square}(174\ \ 57)^{\circ}_{\square}(57\ \ 66)^{\circ}_{\square}(66\ \ 9)^{\circ}_{\square}$	(9 126 117 174 57 66)
$(10\ \ 140)^{\square}_{\circ}(140\ \ 130)^{\square}_{\square}(130\ \ 173)^{\square}_{\circ}(173\ \ 43)^{\square}_{\square}(43\ \ 53)^{\square}_{\circ}(53\ \ 10)^{\square}_{\square}$	(10 140 130 173 43 53)
$(11\ \ 154)^{\square}_{\bullet}(154\ \ 143)^{\square}_{\square}(143\ \ 172)^{\square}_{\bullet}(172\ \ 29)^{\square}_{\square}(29\ \ 40)^{\square}_{\bullet}(40\ \ 11)^{\square}_{\square}$	(11 154 143 172 29 40)
$(12\ \ 168)^{\circ}_{\square}(168\ \ 156)^{\square}_{\square}(156\ \ 171)^{\circ}_{\square}(171\ \ 15)^{\square}_{\square}(15\ \ 27)^{\circ}_{\square}(27\ \ 12)^{\square}_{\square}$	(12 168 156 171 15 27)
$(16\ \ 41)^{\square}_{\circ}(41\ \ 25)^{\square}_{\square}(25\ \ 167)^{\square}_{\circ}(167\ \ 142)^{\square}_{\square}(142\ \ 158)^{\square}_{\circ}(158\ \ 16)^{\square}_{\square}$	(16 41 25 167 142 158)
$(17\ \ 55)^{\bullet}_{\square}(55\ \ 38)^{\square}_{\circ}(38\ \ 166)^{\bullet}_{\square}(166\ \ 128)^{\square}_{\circ}(128\ \ 145)^{\bullet}_{\square}(145\ \ 17)^{\square}_{\circ}$	(17 55 38 166 128 145)
$(18\ \ 69)^{\circ}_{\square}(69\ \ 51)^{\circ}_{\square}(51\ \ 165)^{\circ}_{\square}(165\ \ 114)^{\circ}_{\square}(114\ \ 132)^{\circ}_{\square}(132\ \ 18)^{\circ}_{\square}$	(18 69 51 165 114 132)
$(19\ \ 83)^{\square}_{\circ}(83\ \ 64)^{\square}_{\square}(64\ \ 164)^{\square}_{\circ}(164\ \ 100)^{\square}_{\square}(100\ \ 119)^{\square}_{\circ}(119\ \ 19)^{\square}_{\square}$	(19 83 64 164 100 119)
$(20\ \ 97)^{\bullet}_{\square}(97\ \ 77)^{\square}_{\square}(77\ \ 163)^{\bullet}_{\square}(163\ \ 86)^{\square}_{\square}(86\ \ 106)^{\bullet}_{\square}(106\ \ 20)^{\square}_{\square}$	(20 97 77 163 86 106)
$(21\ \ 111)^{\circ}_{\square}(111\ \ 90)^{\square}_{\square}(90\ \ 162)^{\circ}_{\square}(162\ \ 72)^{\square}_{\square}(72\ \ 93)^{\circ}_{\square}(93\ \ 21)^{\square}_{\square}$	(21 111 90 162 72 93)
$(22\ \ 125)^{\square}_{\square}(125\ \ 103)^{\bullet}_{\square}(103\ \ 161)^{\square}_{\square}(161\ \ 58)^{\bullet}_{\square}(58\ \ 80)^{\square}_{\square}(80\ \ 22)^{\bullet}_{\square}$	(22 125 103 161 58 80)
$(23\ \ 139)^{\square}_{\square}(139\ \ 116)^{\square}_{\circ}(116\ \ 160)^{\square}_{\square}(160\ \ 44)^{\square}_{\circ}(44\ \ 67)^{\square}_{\square}(67\ \ 23)^{\square}_{\circ}$	(23 139 116 160 44 67)
$(24\ \ 153)^{\circ}_{\square}(153\ \ 129)^{\square}_{\square}(129\ \ 159)^{\circ}_{\square}(159\ \ 30)^{\square}_{\square}(30\ \ 54)^{\circ}_{\square}(54\ \ 24)^{\square}_{\square}$	(24 153 129 159 30 54)
$(31\ \ 68)^{\square}_{\square}(68\ \ 37)^{\square}_{\bullet}(37\ \ 152)^{\square}_{\square}(152\ \ 115)^{\square}_{\bullet}(115\ \ 146)^{\square}_{\square}(146\ \ 31)^{\square}_{\bullet}$	(31 68 37 152 115 146)
$(32\ \ 82)^{\square}_{\square}(82\ \ 50)^{\square}_{\circ}(50\ \ 151)^{\square}_{\square}(151\ \ 101)^{\square}_{\circ}(101\ \ 133)^{\square}_{\square}(133\ \ 32)^{\square}_{\circ}$	(32 82 50 151 101 133)
$(33\ \ 96)^{\circ}_{\square}(96\ \ 63)^{\square}_{\square}(63\ \ 150)^{\circ}_{\square}(150\ \ 87)^{\square}_{\square}(87\ \ 120)^{\circ}_{\square}(120\ \ 33)^{\square}_{\square}$	(33 96 63 150 87 120)
$(34\ \ 110)^{\square}_{\circ}(110\ \ 76)^{\square}_{\square}(76\ \ 149)^{\square}_{\circ}(149\ \ 73)^{\square}_{\square}(73\ \ 107)^{\square}_{\circ}(107\ \ 34)^{\square}_{\square}$	(34 110 76 149 73 107)
$(35\ \ 124)^{\square}_{\square}(124\ \ 89)^{\square}_{\circ}(89\ \ 148)^{\square}_{\square}(148\ \ 59)^{\square}_{\circ}(59\ \ 94)^{\square}_{\square}(94\ \ 35)^{\square}_{\circ}$	(35 124 89 148 59 94)
$(36\ \ 138)^{\square}_{\square}(138\ \ 102)^{\circ/\bullet}_{\square}(102\ \ 147)^{\square}_{\square}(147\ \ 45)^{\circ/\bullet}_{\square}(45\ \ 81)^{\square}_{\square}(81\ \ 36)^{\circ/\bullet}_{\square}$	(36 138 102 147 45 81)
$(46\ \ 95)^{\square}_{\square}(95\ \ 49)^{\bullet}_{\square}(49\ \ 137)^{\square}_{\square}(137\ \ 88)^{\bullet}_{\square}(88\ \ 134)^{\square}_{\square}(134\ \ 46)^{\bullet}_{\square}$	(46 95 49 137 88 134)
$(47\ \ 109)^{\square}_{\bullet}(109\ \ 62)^{\square}_{\circ}(62\ \ 136)^{\square}_{\bullet}(136\ \ 74)^{\square}_{\circ}(74\ \ 121)^{\square}_{\bullet}(121\ \ 47)^{\square}_{\circ}$	(47 109 62 136 74 121)
$(48\ \ 123)^{\circ}_{\square}(123\ \ 75)^{\circ}_{\square}(75\ \ 135)^{\circ}_{\square}(135\ \ 60)^{\circ}_{\square}(60\ \ 108)^{\circ}_{\square}(108\ \ 48)^{\circ}_{\square}$	(48 123 75 135 60 108)
$(61\ \ 122)^{\square}_{\bullet}(122\ \ 61)^{\square}_{\bullet}$	(61 122)

1.2.2 Site occupancy scheme in 'linear shift' representation

$(X\ \ Y)^{F1}_{F2}$		
(0 0)$^{\bullet}_{\square}$	(1 14)$^{\square}_{\circ}$	(2 28)$^{\square}_{\square}$
(3 42)$^{\square}_{\square}$	(4 56)$^{\square}_{\circ}$	(5 70)$^{\square}_{\bullet}$
(6 84)$^{\circ}_{\square}$	(7 98)$^{\square}_{\circ}$	(8 112)$^{\square}_{\bullet}$
(9 126)$^{\circ}_{\square}$	(10 140)$^{\square}_{\circ}$	(11 154)$^{\square}_{\bullet}$
(12 168)$^{\circ}_{\square}$	(13 182)$^{\square}_{\circ}$	(14 13)$^{\bullet}_{\square}$
(15 27)$^{\circ}_{\square}$	(16 41)$^{\square}_{\circ}$	(17 55)$^{\bullet}_{\square}$
(18 69)$^{\circ}_{\square}$	(19 83)$^{\square}_{\circ}$	(20 97)$^{\bullet}_{\square}$
(21 111)$^{\circ}_{\square}$	(22 125)$^{\square}_{\square}$	(23 139)$^{\square}_{\square}$
(24 153)$^{\circ}_{\square}$	(25 167)$^{\square}_{\circ}$	(26 181)$^{\square}_{\square}$
(27 12)$^{\square}_{\square}$	(28 26)$^{\square}_{\circ}$	(29 40)$^{\square}_{\bullet}$
(30 54)$^{\circ}_{\square}$	(31 68)$^{\square}_{\square}$	(32 82)$^{\square}_{\square}$
(33 96)$^{\circ}_{\square}$	(34 110)$^{\square}_{\circ}$	(35 124)$^{\square}_{\square}$
(36 138)$^{\square}_{\square}$	(37 152)$^{\square}_{\square}$	(38 166)$^{\bullet}_{\square}$
(39 180)$^{\square}_{\square}$	(40 11)$^{\square}_{\square}$	(41 25)$^{\square}_{\square}$
(42 39)$^{\circ}_{\square}$	(43 53)$^{\square}_{\circ}$	(44 67)$^{\square}_{\square}$
(45 81)$^{\square}_{\square}$	(46 95)$^{\square}_{\square}$	(47 109)$^{\square}_{\bullet}$
(48 123)$^{\circ}_{\square}$	(49 137)$^{\square}_{\square}$	(50 151)$^{\square}_{\square}$
(51 165)$^{\circ}_{\square}$	(52 179)$^{\square}_{\circ}$	(53 10)$^{\square}_{\square}$
(54 24)$^{\square}_{\square}$	(55 38)$^{\square}_{\circ}$	(56 52)$^{\bullet}_{\square}$
(57 66)$^{\circ}_{\square}$	(58 80)$^{\square}_{\square}$	(59 94)$^{\square}_{\square}$
(60 108)$^{\circ}_{\square}$	(61 122)$^{\square}_{\bullet}$	(62 136)$^{\square}_{\bullet}$
(63 150)$^{\circ}_{\square}$	(64 164)$^{\square}_{\circ}$	(65 178)$^{\square}_{\bullet}$
(66 9)$^{\circ}_{\square}$	(67 23)$^{\square}_{\circ}$	(68 37)$^{\square}_{\bullet}$
(69 51)$^{\circ}_{\square}$	(70 65)$^{\square}_{\circ}$	(71 79)$^{\square}_{\bullet}$
(72 93)$^{\circ}_{\square}$	(73 107)$^{\square}_{\circ}$	(74 121)$^{\square}_{\bullet}$
(75 135)$^{\circ}_{\square}$	(76 149)$^{\square}_{\circ}$	(77 163)$^{\bullet}_{\square}$
(78 177)$^{\circ}_{\square}$	(79 8)$^{\square}_{\circ}$	(80 22)$^{\bullet}_{\square}$
(81 36)$^{\circ/\bullet}_{\square}$	(82 50)$^{\square}_{\circ}$	(83 64)$^{\square}_{\square}$
(84 78)$^{\square}_{\square}$	(85 92)$^{\square}_{\circ}$	(86 106)$^{\bullet}_{\square}$
(87 120)$^{\circ}_{\square}$	(88 134)$^{\square}_{\square}$	(89 148)$^{\square}_{\square}$
(90 162)$^{\circ}_{\square}$	(91 176)$^{\square}_{\circ}$	(92 7)$^{\square}_{\square}$

$(X\ \ Y)^{F1}_{F2}$		
(93 21)$^{\square}_{\square}$	(94 35)$^{\square}_{\circ}$	(95 49)$^{\bullet}_{\square}$
(96 63)$^{\square}_{\square}$	(97 77)$^{\square}_{\square}$	(98 91)$^{\square}_{\square}$
(99 105)$^{\circ}_{\square}$	(100 119)$^{\square}_{\circ}$	(101 133)$^{\square}_{\square}$
(102 147)$^{\square}_{\square}$	(103 161)$^{\square}_{\square}$	(104 175)$^{\square}_{\bullet}$
(105 6)$^{\square}_{\square}$	(106 20)$^{\square}_{\square}$	(107 34)$^{\square}_{\square}$
(108 48)$^{\circ}_{\square}$	(109 62)$^{\square}_{\circ}$	(110 76)$^{\square}_{\square}$
(111 90)$^{\square}_{\square}$	(112 104)$^{\square}_{\circ}$	(113 118)$^{\square}_{\bullet}$
(114 132)$^{\circ}_{\square}$	(115 146)$^{\square}_{\square}$	(116 160)$^{\square}_{\square}$
(117 174)$^{\circ}_{\square}$	(118 5)$^{\square}_{\circ}$	(119 19)$^{\square}_{\square}$
(120 33)$^{\square}_{\square}$	(121 47)$^{\square}_{\circ}$	(122 61)$^{\bullet}_{\square}$
(123 75)$^{\circ}_{\square}$	(124 89)$^{\square}_{\circ}$	(125 103)$^{\bullet}_{\square}$
(126 117)$^{\circ}_{\square}$	(127 131)$^{\square}_{\circ}$	(128 145)$^{\bullet}_{\square}$
(129 159)$^{\circ}_{\square}$	(130 173)$^{\square}_{\circ}$	(131 4)$^{\bullet}_{\square}$
(132 18)$^{\circ}_{\square}$	(133 32)$^{\square}_{\circ}$	(134 46)$^{\bullet}_{\square}$
(135 60)$^{\circ}_{\square}$	(136 74)$^{\square}_{\circ}$	(137 88)$^{\bullet}_{\square}$
(138 102)$^{\circ/\bullet}_{\square}$	(139 116)$^{\square}_{\circ}$	(140 130)$^{\square}_{\square}$
(141 144)$^{\square}_{\square}$	(142 158)$^{\square}_{\circ}$	(143 172)$^{\square}_{\bullet}$
(144 3)$^{\circ}_{\square}$	(145 17)$^{\square}_{\circ}$	(146 31)$^{\square}_{\bullet}$
(147 45)$^{\circ/\bullet}_{\square}$	(148 59)$^{\square}_{\circ}$	(149 73)$^{\square}_{\square}$
(150 87)$^{\square}_{\square}$	(151 101)$^{\square}_{\circ}$	(152 115)$^{\square}_{\bullet}$
(153 129)$^{\square}_{\square}$	(154 143)$^{\square}_{\square}$	(155 157)$^{\square}_{\square}$
(156 171)$^{\circ}_{\square}$	(157 2)$^{\square}_{\circ}$	(158 16)$^{\square}_{\square}$
(159 30)$^{\square}_{\square}$	(160 44)$^{\square}_{\circ}$	(161 58)$^{\bullet}_{\square}$
(162 72)$^{\square}_{\square}$	(163 86)$^{\square}_{\square}$	(164 100)$^{\square}_{\square}$
(165 114)$^{\circ}_{\square}$	(166 128)$^{\square}_{\circ}$	(167 142)$^{\square}_{\square}$
(168 156)$^{\square}_{\square}$	(169 170)$^{\square}_{\circ}$	(170 1)$^{\bullet}_{\square}$
(171 15)$^{\square}_{\square}$	(172 29)$^{\square}_{\square}$	(173 43)$^{\square}_{\square}$
(174 57)$^{\circ}_{\square}$	(175 71)$^{\square}_{\circ}$	(176 85)$^{\square}_{\square}$
(177 99)$^{\square}_{\square}$	(178 113)$^{\square}_{\circ}$	(179 127)$^{\bullet}_{\square}$
(180 141)$^{\circ}_{\square}$	(181 155)$^{\square}_{\circ}$	(182 169)$^{\bullet}_{\square}$

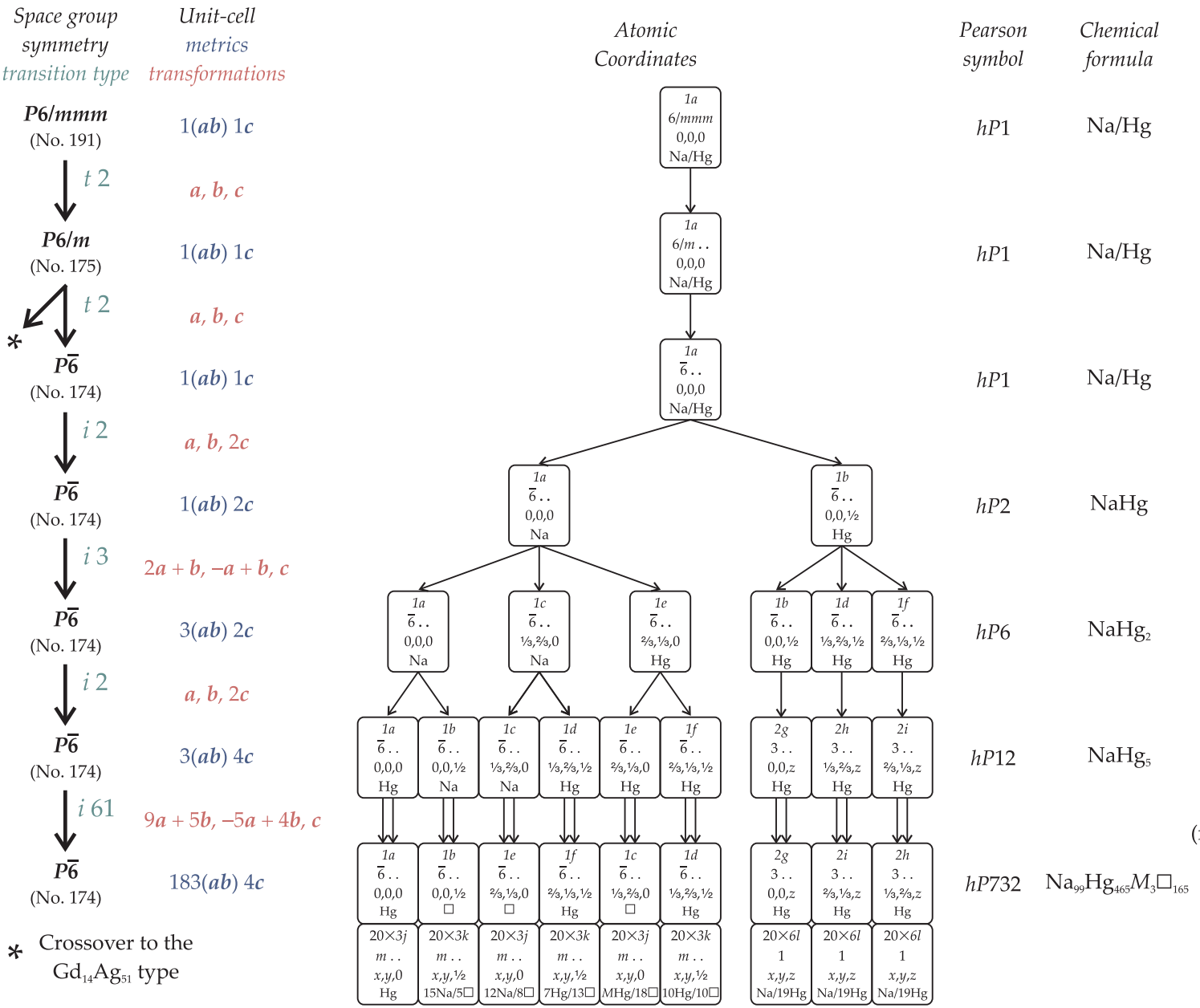
Space group symmetry transition type
Unit-cell metrics transformations
Atomic Coordinates
Pearson symbol
Chemical formula
Chemical reason for symmetry reduction
P6/mmm (No. 191)
1(ab) 1c
hP1
Na/Hg
t 2
a, b, c
P6/m (No. 175)
1(ab) 1c
hP1
Na/Hg
Two steps of site symmetry reduction
t 2
a, b, c
*
P6̄ (No. 174)
1(ab) 1c
hP1
Na/Hg
i 2
a, b, 2c
P6̄ (No. 174)
1(ab) 2c
hP2
NaHg
Ordering of atomic species
i 3
2a + b, −a + b, c
P6̄ (No. 174)
3(ab) 2c
hP6
NaHg2
1st sublattice generation (Na2Hg ordering)
i 2
a, b, 2c
P6̄ (No. 174)
3(ab) 4c
hP12
NaHg5
Doubling in c, puckering in z
i 61
9a + 5b, −5a + 4b, c
P6̄ (No. 174)
183(ab) 4c
hP732
Na99Hg465M3□165
2nd sublattice generation (mainly vacancy formation)
* Crossover to the Gd14Ag51 type

2 Remarks on the diffraction pattern of $Na_{11}Hg_{52}$

2.1 Selected reciprocal space sections of $Na_{11}Hg_{52}$

Here we show reconstructed sections of reciprocal space from the actual diffraction experiment performed on $Na_{11}Hg_{52}$, which formed the basis for the single-crystal structure solution and refinement of its crystal structure. The keen crystallographer will possibly find quite a few telltale signs of peculiar diffraction phenomena, of which reflections located at *wavy* 'lattice lines' appear to be the most obvious (see $h2l$ in particular), thereby hinting at some possible description as an incommensurately modulated phase. However, the real intention of showing these reciprocal sections is an aesthetical rather than a scientific one: Have fun, while pondering about them!

Figure 1: Reciprocal space sections of $Na_{11}Hg_{52}$: $hk0$.

Figure 2: Reciprocal space sections of $Na_{11}Hg_{52}$: hkl to $hk6$.

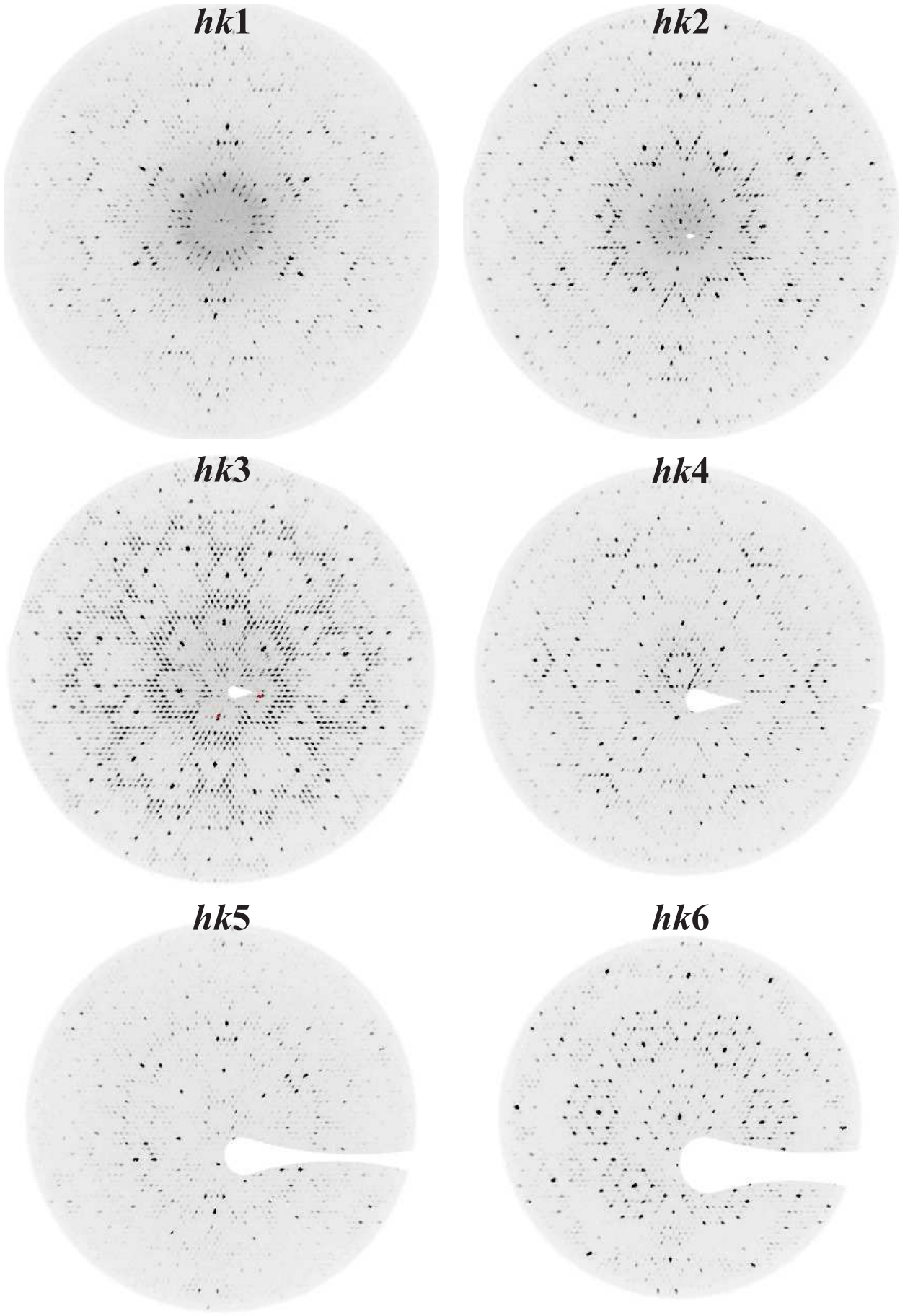

Figure 3: Reciprocal space sections of $Na_{11}Hg_{52}$: $h0l$ to $h4l$.

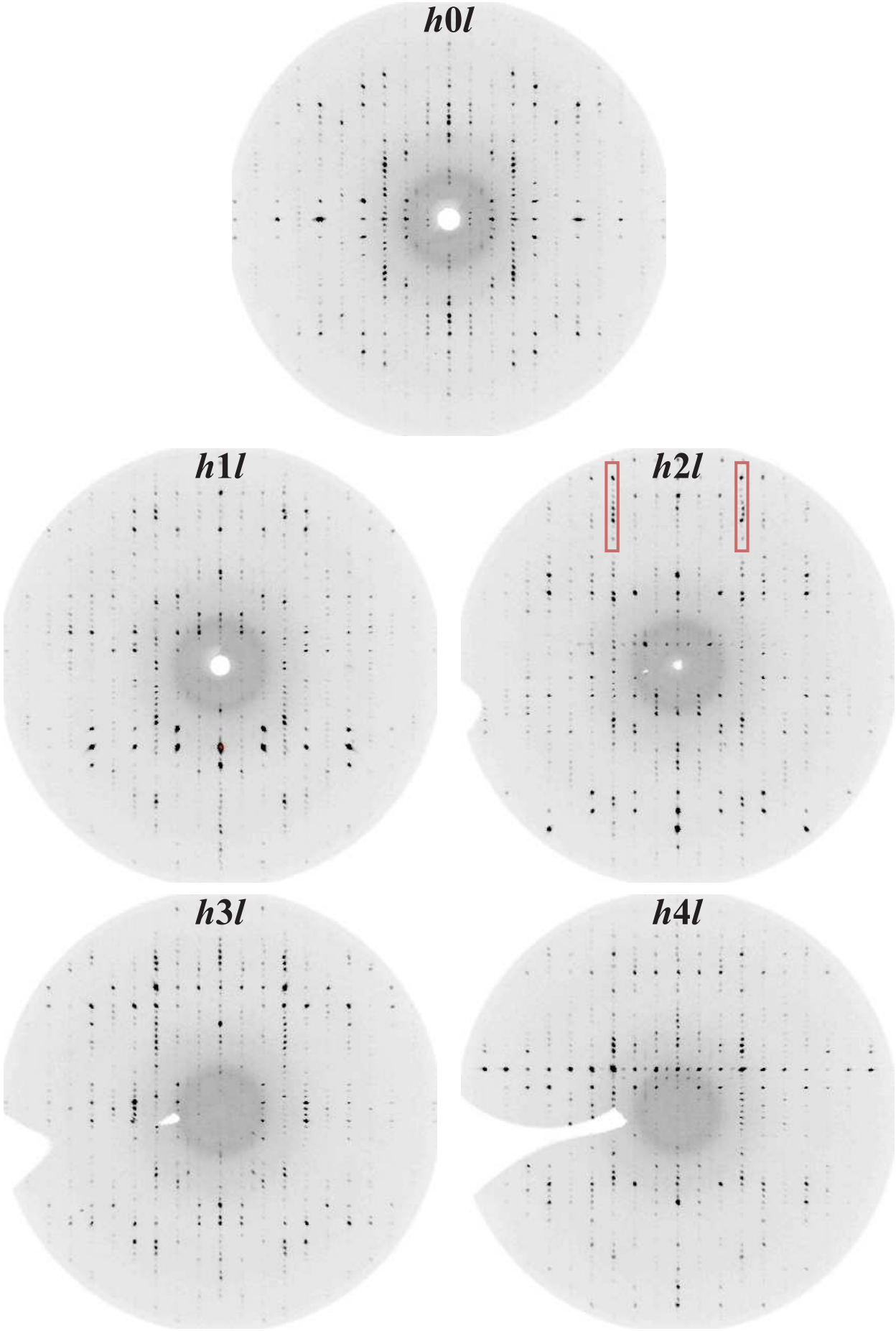

Figure 4: Reciprocal space sections of $Na_{11}Hg_{52}$: $0kl$ to $4kl$.

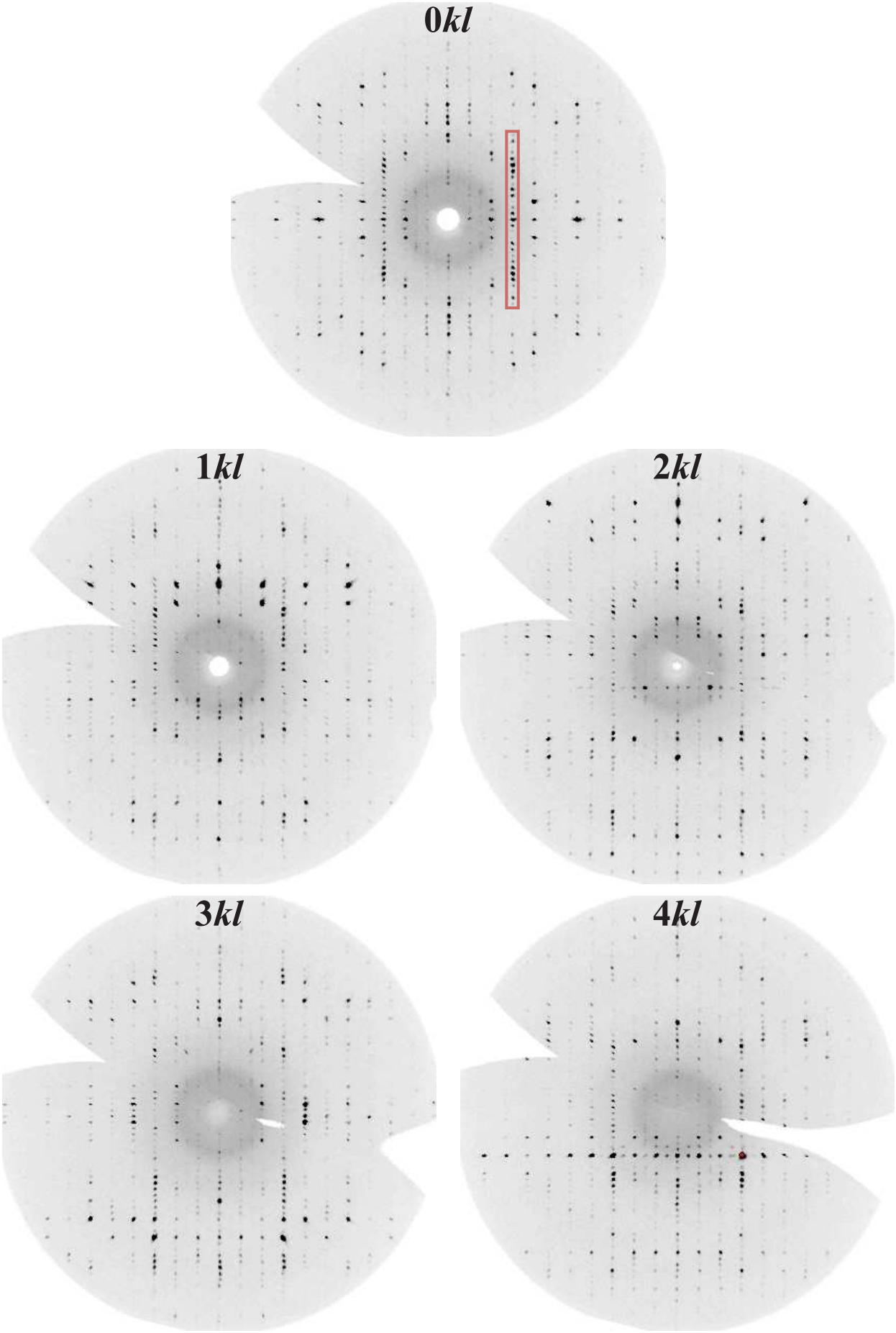

2.2 Schematic diffraction patterns $hk0$ of sublattices and partial structures used for the description of $Na_{11}Hg_{52}$

In the following we show a collection of schematic diffraction patterns calculated for two-dimensional real space projections $xy0$ of point patterns (shown within a unit square) and their corresponding reciprocal space sections $hk0$. Intensities were calculated according to the formula:

$$I_{hk} = S \cdot \left| \sum_{j=1}^{N} f_j \cdot \exp\left[2\pi\, i\, (hx_j + ky_j)\right] \right|^2 , \tag{1}$$

where S is an arbitrary scaling factor (with values given for relative comparison) and f_j was set to unity for all patterns, irrespective of the nature (Na or Hg) of the point scatterer.[1] Reciprocal space sections are shown for $|h + k| \leqslant 40$.

The purpose of this presentation is twofold, being didactic on the one hand, by means of highlighting the diffracion signatures of a selection of idealized superlattices in general, and pragmatic on the other hand, in order to separate the individual scattering contributions of these sublattices with respect to the diffraction pattern of $Na_{11}Hg_{52}$. Although the actual reciprocal space intensity distribution is determined by the interplay of all partial structures, especially including all the actual deviations from the idealized description, the influence of the superstructure ordering remains strong enough to discern it in the diffraction pattern.

A note on the following (ab)use of language: *Ideal* designates a full sublattice (i.e. with all possible sites occupied), whereas *actual* denotes a defective one; yet even the defective sublattices are themselves idealizations to the actual crystal structure!

[1] Indeed, the diffraction from the appropriate union of partial structures, even if accounted for the strong difference in scattering contrast of Na and Hg, is dominated by the spatial perfection of the idealized sublattice with $T(14, 1) = 183$. This means, that almost all of the actually observable detailed features of the diffraction pattern (in all their subtlety and splendour) result from deviations from the perfect order of the ideal sublattice.

Figure 5: Ideal sublattice $T(14,1) = 183$, $Y \equiv 14\,X \pmod{183}$ (top left); Ideal sublattice $T(9,5) = 169$, $Y \equiv 147\,X \pmod{169}$ (top right); Both aforementioned ideal sublattices combined (bottom left); Ideal sublattice $T(9,5) = 61$, $Y \equiv 14\,X \pmod{61}$ (bottom right). $S = 2 \times 10^{-4}$ always. Apart from the superstructure reflections reciprocal lattice points are highlighted and should not to be mistaken for intensities!

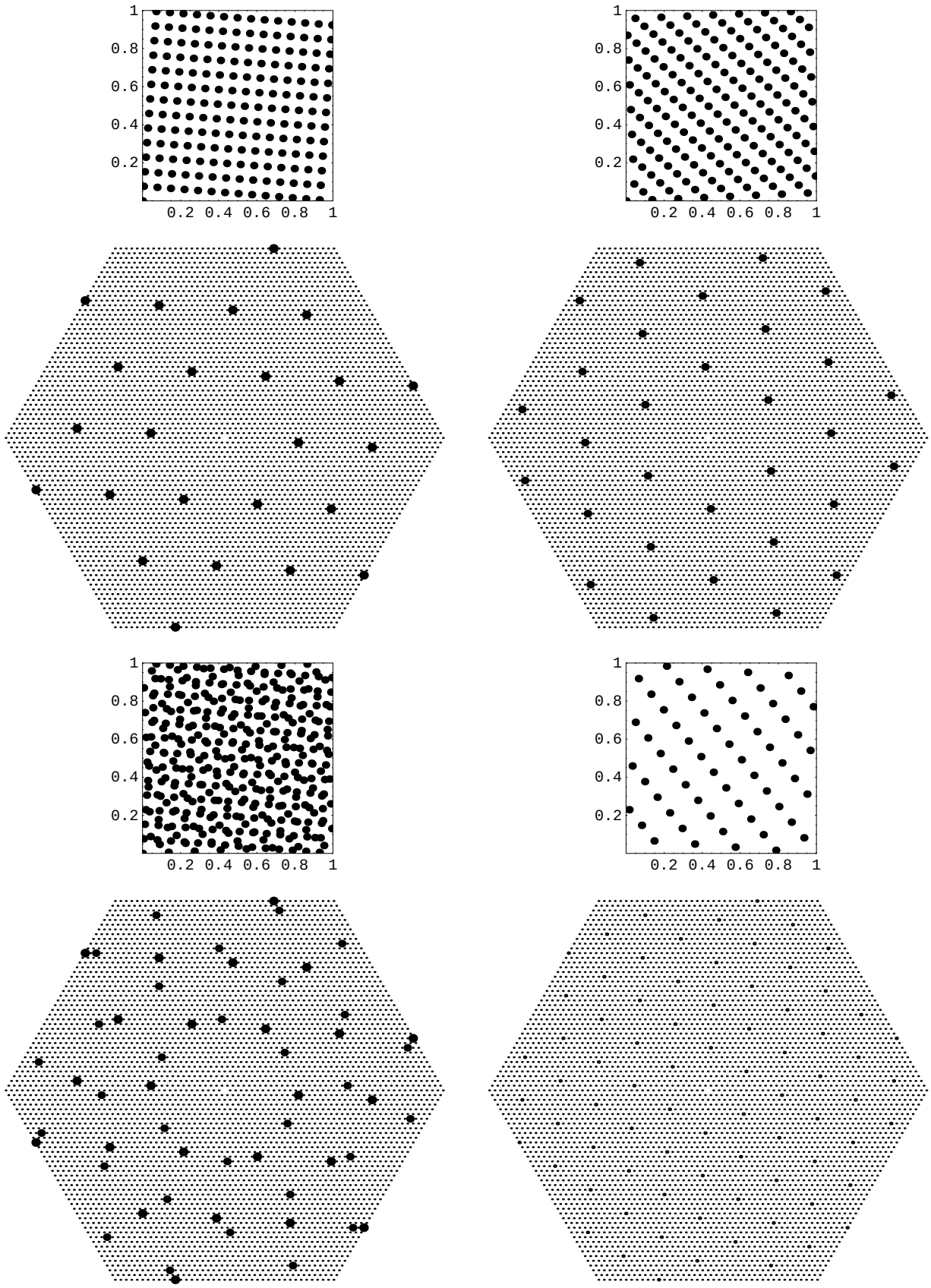

Figure 6: Ideal Na-substructure of the combined $F12_{183}$-layers (top left, $S = 6 \times 10^{-4}$); Ideal Hg-substructure of the combined $F12_{183}$-layers (top right, $S = 6 \times 10^{-4}$); Actual Na-substructure of the combined $F12_{183}$-layers (bottom left, $S = 6 \times 10^{-4}$); Actual Hg-substructure of the combined $F12_{183}$-layers (bottom right, $S = 6 \times 10^{-3}$!).

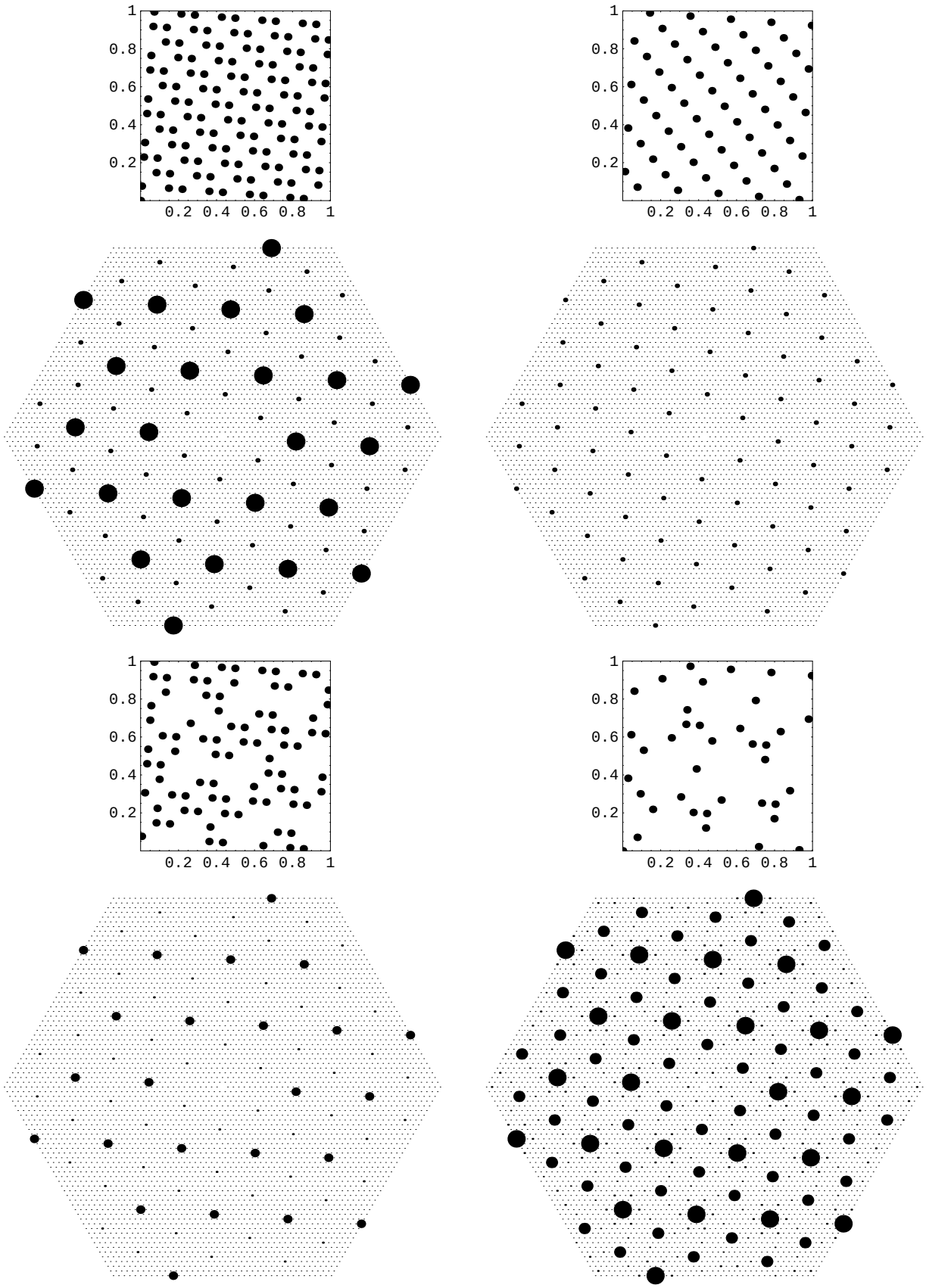

Figure 7: Actual Na-substructure of the P-layers (top left, $S = 6 \times 10^{-2}$); Actual Hg-substructure of the P-layers (top right, $S = 2 \times 10^{-4}$); Actual Na- and Hg-substructure of the combined $F12_{183}$-layers (bottom left, $S = 2 \times 10^{-4}$); Actual Hg-substructure of the combined $F12_{169}$-layers, with the second one shifted as described in the main body of the article (bottom right, $S = 2 \times 10^{-3}$).

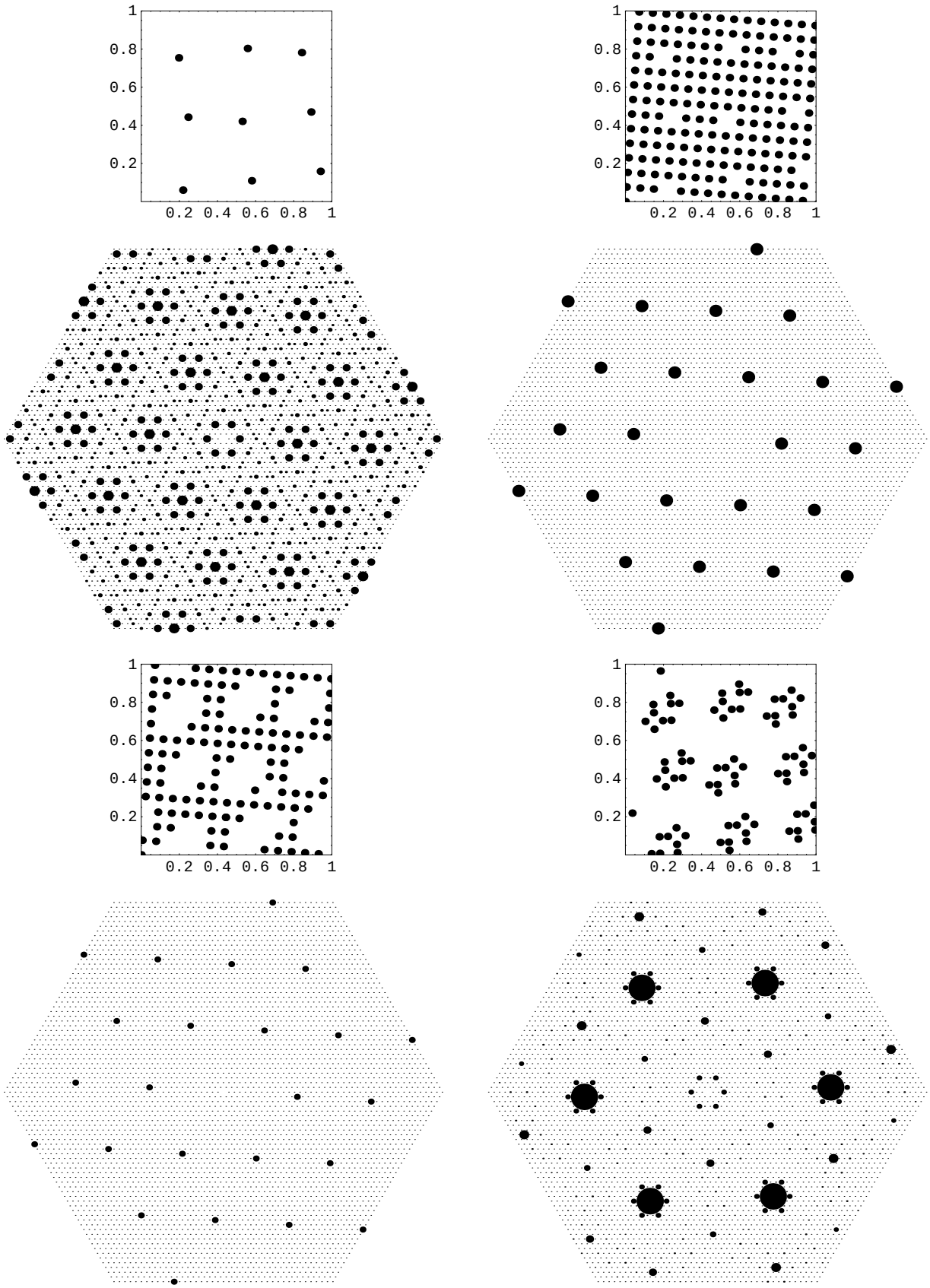

3 Selection of enlarged figures

Here, we show a few of the more complicated figures from the main article, especially concerned with the occupation of sublattice sites by sodium (lightgray) or mercury (darkgray) atoms.

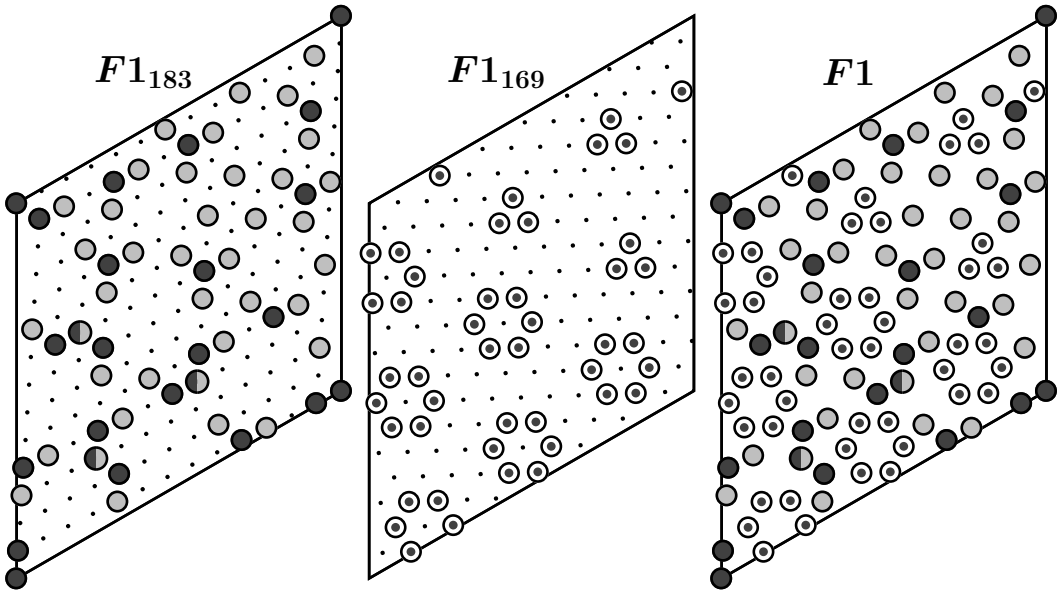

Figure 8: Idealized description of the $F1$-layer by *two* sublattices of index $T(14,1) = 183$ (left) and $T(15,7) = 169$ (middle) and their combination (right).

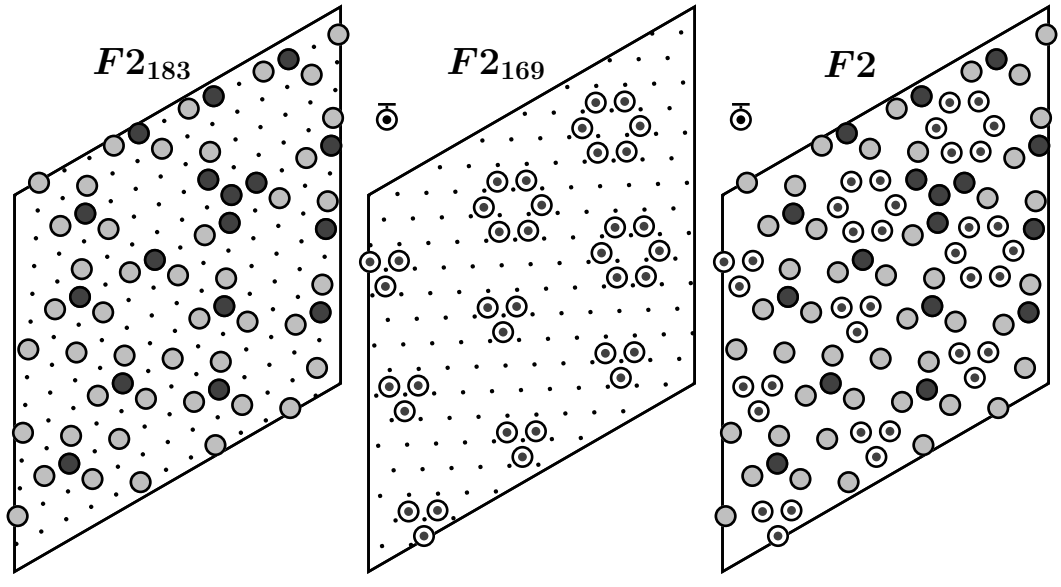

Figure 9: Idealized description of the $F2$-layer by *two* sublattices of index $T(14,1) = 183$ (left) and $T(15,7) = 169$ (middle) and their combination (right).

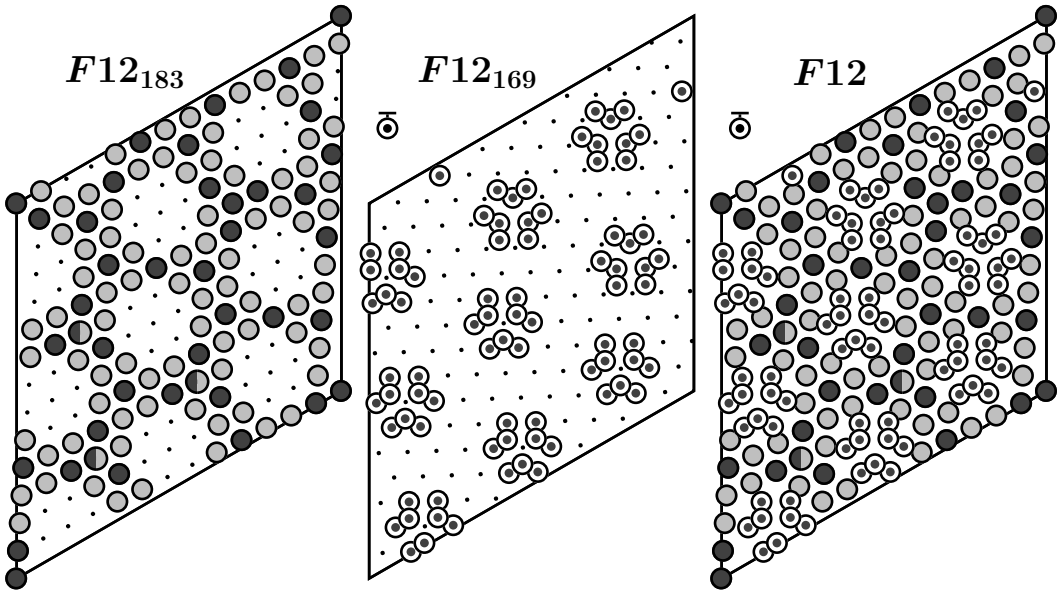

Figure 10: Combination of the idealized descriptions of the $F1$- and $F2$-layer by *two* sublattices of index $T(14,1) = 183$ (left) and $T(15,7) = 169$ (middle) and their meta-combination (right).

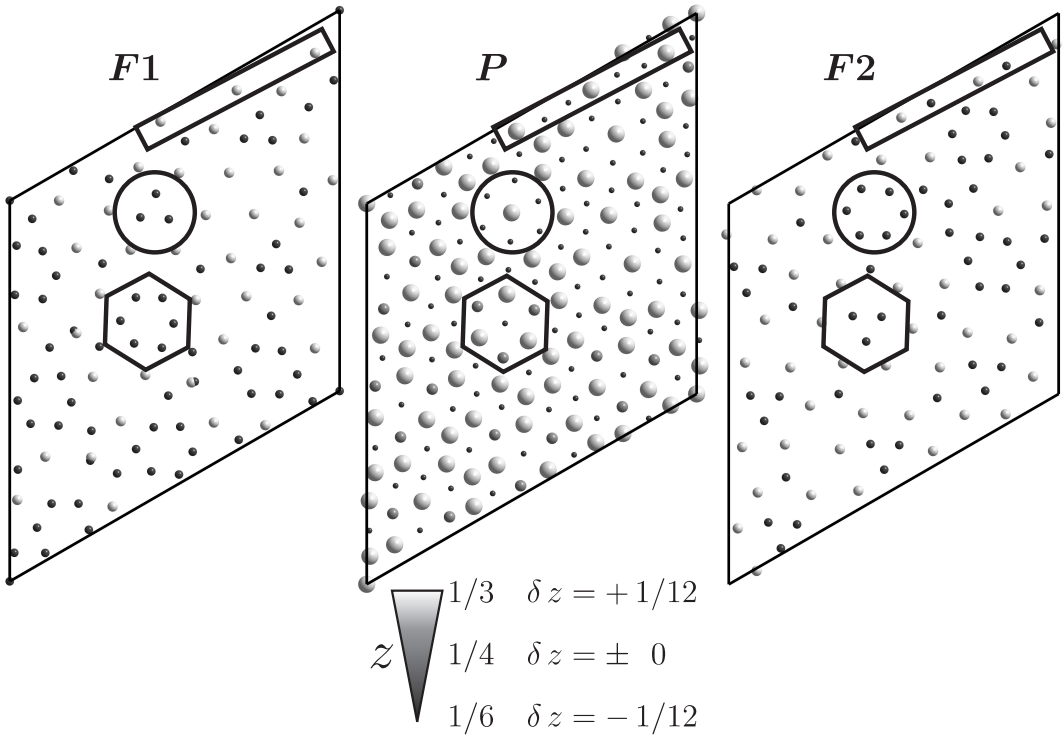

Figure 11: Structural correlation of the puckering of the P-layer (middle) with the occupancy of the adjacent $F1/F2$-layers (left and right). Note, that the radii and gray values of the atoms within the P-layers do not represent the chemical decoration of the sublattice sites but instead denote the approximate height of the atoms in the z-direction, allowing for the depiction of atomic displacements $\delta z = \pm 1/12$ relative to the average height of the P-layer at $\langle z \rangle = 1/4$.

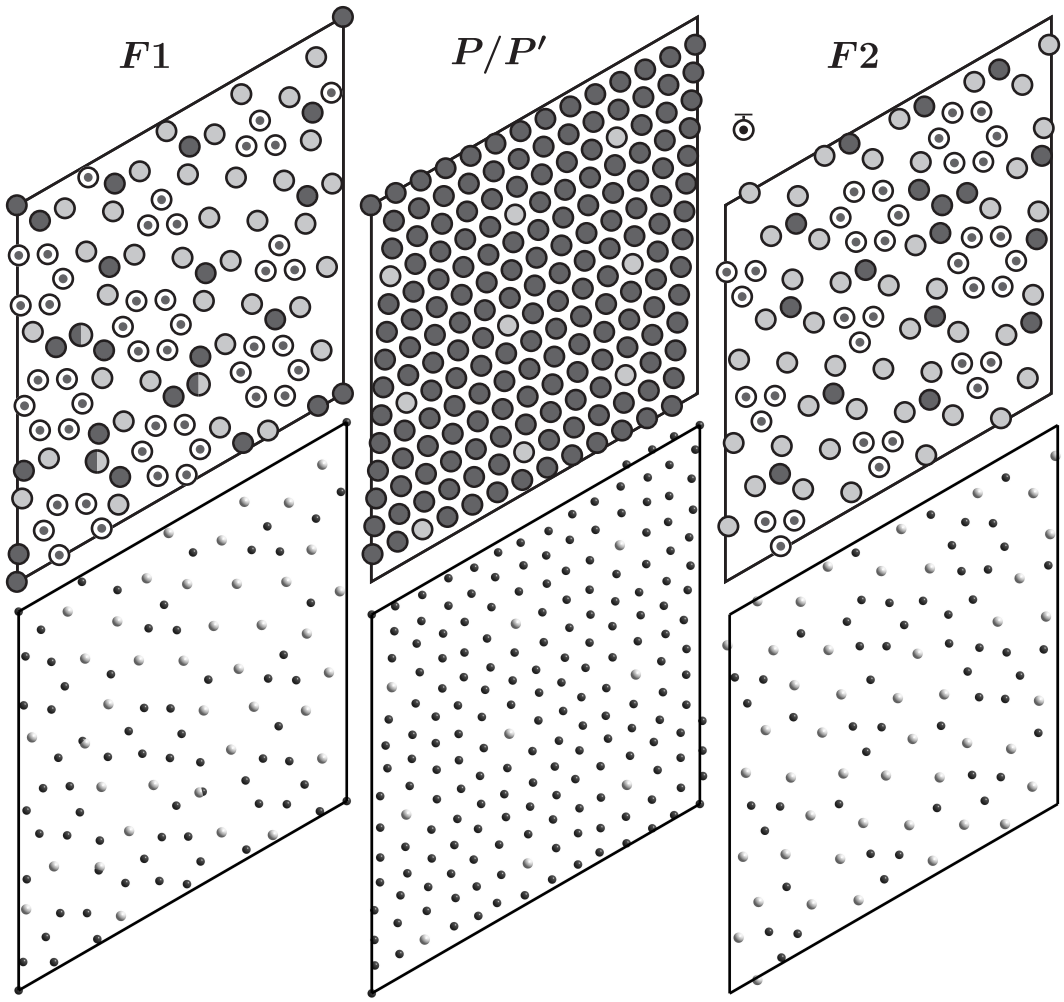

Figure 12: Comparison of the idealized layers (top) to the actual ones (bottom). Although slight deviations occur, the distribution of Na- and Hg-atoms is described quite well using sublattices and their MCG-encoding.